



ELSEVIER

Thermochimica Acta 263 (1995) 29–50

thermochimica
acta

Prediction of the thermal response of hazardous materials during storage using an improved technique

Johannes Opfermann^{a,*}, Winfried Hädrich^b

^a*Netzsch-Gerätebau GmbH, D-95100 Selb, Germany*

^b*Sandoz Technologie AG, CH-4002 Basel, Switzerland*

Received 9 January 1995; accepted 24 March 1995

Abstract

In order to achieve predictions with a high degree of confidence concerning the thermal behaviour of high-energy materials, the heat-generating process in the inhomogenous thermal conduction equation is described by a one- to four-step reaction process. Deconvolution and kinetic analysis, using multivariate non-linear regression of DSC measurements together provide the basis for relevant kinetic parameters to describe the thermal behaviour of Zoalen above the melting temperature. It is shown that only when one has a combination of DSC measurements and measurements with highly-sensitive micro calorimeters, can predictions with a high degree of confidence be achieved over the entire temperature range.

Keywords: DSC; Microcalorimetry; Multiple step decomposition kinetics; Simulation

1. Introduction

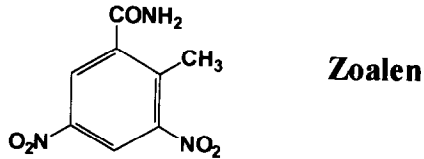
Materials with a high exothermal decomposition potential are liable to explode under certain conditions. In this category, solid materials are particularly dangerous when the decomposition starts below the melting temperature. Due to the insufficient convection and the limited thermal conductivity, a progressive temperature increase can easily take place, resulting in a thermal explosion.

Frequent observations show that kinetic decomposition often changes with the temperature. This happens when the decomposition process is multistaged and, as a function of temperature and/or time, the step which determines speed shifts to another stage.

* Corresponding author.

All known theories and also more recent papers [1,2] take into account only one-step reactions for the heat generating process. The correct description of the decomposition process is the essential basis of an accurate prediction. It is therefore of great importance from the point of view of safety regulations, when the known theory can be extended to include a description of the decomposition process by more complex reactions.

On the other hand, the simulation can be very closely fitted to the surrounding conditions by free selection of heat capacity, heat conductivity and heat dissipation over the surface. In this way, even borderline cases are made accessible to adiabatic behaviour.



“Zoalen” (3,5-dinitro-*o*-toluamide) is a model substance which has proved ideal for testing this programme because:

- the decomposition potential is very high, 3000 J/g
- the decomposition kinetics are relatively complex
- an exothermal decomposition can be determined with highly sensitive microcalorimeters, even at more than 100°C below the melting point
- Zoalen caused a bad explosion in England during the 1970s. By comparing the simulation results with the facts that were gathered after the explosion, the algorithms’ efficiency can be checked.

2. Theory

The following three models are mostly used to describe the kinetics of self-initiated thermal explosions [3,4]. They differ in special assumptions which usually simplify the solutions.

2.1. Semenov model

The Semenov model [5,6] assumes a steady temperature distribution within the reactant. This heat is dissipated over the surface according to Newton’s law, i.e. proportionally to the difference between the surface temperature T_s and the surrounding temperature T_a (Eq. 1). The uniform temperature distribution is produced by assuming an infinite thermal conductivity. This model is therefore correct for an ideal mixture of reactants with finite thermal conduction over the surface.

$$\overline{\rho \cdot c_v} \cdot \frac{\partial T}{\partial t} - k(T_s - T_a) = (-\Delta H) \cdot f(c, T) \quad (1)$$

2.2. Frank-Kamenetskii model

The Frank-Kamenetskii [7] model takes the finite thermal conductivity in a reactant into consideration but assumes, on the other hand, an infinitely high heat exchange over the surface of the reactor, so that the surface temperature of the reactor T_s is equal to the surrounding temperature T_a (equation 2).

$$\lambda \left(\frac{\partial^2 T}{\partial r^2} + \frac{j}{r} \frac{\partial T}{\partial r} \right) + \frac{1}{\rho \cdot c_v} \cdot \frac{\partial T}{\partial t} = (-\Delta H) \cdot f(c, T) \quad (2)$$

The following boundary conditions are valid:

$$T = T_a \quad \text{for } r = R_0 \quad (2a)$$

$$\frac{\partial T}{\partial r} = 0 \quad \text{for } r = 0 \quad (2b)$$

2.3. Thomas model

The Thomas model [8] describes the thermal behaviour according to Newton's law, considering the finite thermal conductivity of the reactant and the heat exchange over the surface. This model allows quite a good fitting with the real conditions and contains both previously mentioned models as boundaries.

$$\lambda \left(\frac{\partial^2 T}{\partial r^2} + \frac{j}{r} \frac{\partial T}{\partial r} \right) + \frac{1}{\rho \cdot c_v} \cdot \frac{\partial T}{\partial t} = (-\Delta H) \cdot f(c, T) \quad (3)$$

The following boundary conditions are valid:

$$-\lambda \left(\frac{\partial T}{\partial r} \right) = k \cdot (T_s - T_a) \quad \text{for } r = R_0 \quad (3a)$$

$$\frac{\partial T}{\partial r} = 0 \quad \text{for } r = 0 \quad (3b)$$

The following nomenclature is valid for all models:

ρ	density of the reactants in g cm^{-3}
c_v	specific heat in J (g K)^{-1}
λ	thermal conductivity in W (cm K)^{-1}
r	radial distance from the centre in cm
R_0	the radius of the cylinder or the sphere in cm
$T(r)$	temperature at the distance r from the centre in $^\circ\text{C}$
T_s	surface temperature of the reactor in $^\circ\text{C}$

T_a	surrounding temperature in °C
T_0	273.15°C
$-\Delta H$	the reaction heat in J g ⁻¹ which is set free during decomposition
j	a geometry factor which is dependent on the type of reactor: $j = 0$ for the infinite plate; $j = 1$ for the infinite cylinder; $j = 2$ for the sphere
k	the surface heat transfer coefficient (transfer coefficient) in W (cm ² K) ⁻¹
$f(c, T)$	the law of formation for the generation of heat for which, up to now, a one-step reaction of the n th order was assumed for all three models. The temperature dependence here is described by an Arrhenius equation (Eq. 4):

$$f(c, T) = (c/c_0)^n A \exp(-E/RT) \quad (4)$$

c/c_0	relative concentration of the reactant
n	reaction order
A	pre-exponential factor in s ⁻¹
E	activation energy in kJ mol ⁻¹
R	gas constant = 8.314 J (mol K) ⁻¹

2.4. Extension of the Thomas model

A condition has been achieved with the Thomas model in which the external conditions are largely taken into consideration. However, for the heat generating process, fundamental simplifications were made, i.e. that the reaction process is one-step and can be described by a reaction of n th order, the temperature dependence of which follows the Arrhenius equation (Eq. 4).

Experience in kinetic analysis now shows that, in general, the assumption of a one-step reaction does not apply. It is true that, under certain conditions, a reaction step is often a speed controlling factor, but which reaction step of a complex reaction this actually is, depends on the prevailing conditions. The weighting can also shift from one reaction step to another. Therefore, one should not presume from the outset that the reduction of the model of the decomposition kinetics to a one-step reaction is an acceptable simplification. There is no doubt that an adequate description of the decomposition kinetics under different conditions is an absolute prerequisite for a prediction which has any acceptable degree of confidence. Therefore the logical consequence is that the Thomas model, which is actually the most adjustable to reality, should be extended to include the possibility of describing the heat generating process by multiple step reactions.

Analog to the programme "NETZSCH Thermokinetic Analysis, MultipleScan" [9,10], the Thomas model is now so expanded that it can also describe the heat generating decomposition process, by up to four-step reactions. Independent, competitive and following reactions are possible here in different combinations (Figs. 1 and 2). Every reaction step of a model can be characterized by the reaction types shown in Table 1. These reaction types contain both normal elementary reactions, such as a reaction of the first, second or n th order, and also typical solid state reactions, such as phase boundary reactions or diffusion reactions of different dimensions. The relative concentration c/c_0 is shown here by the degree of conversion, as is usual with solid state reactions [11].

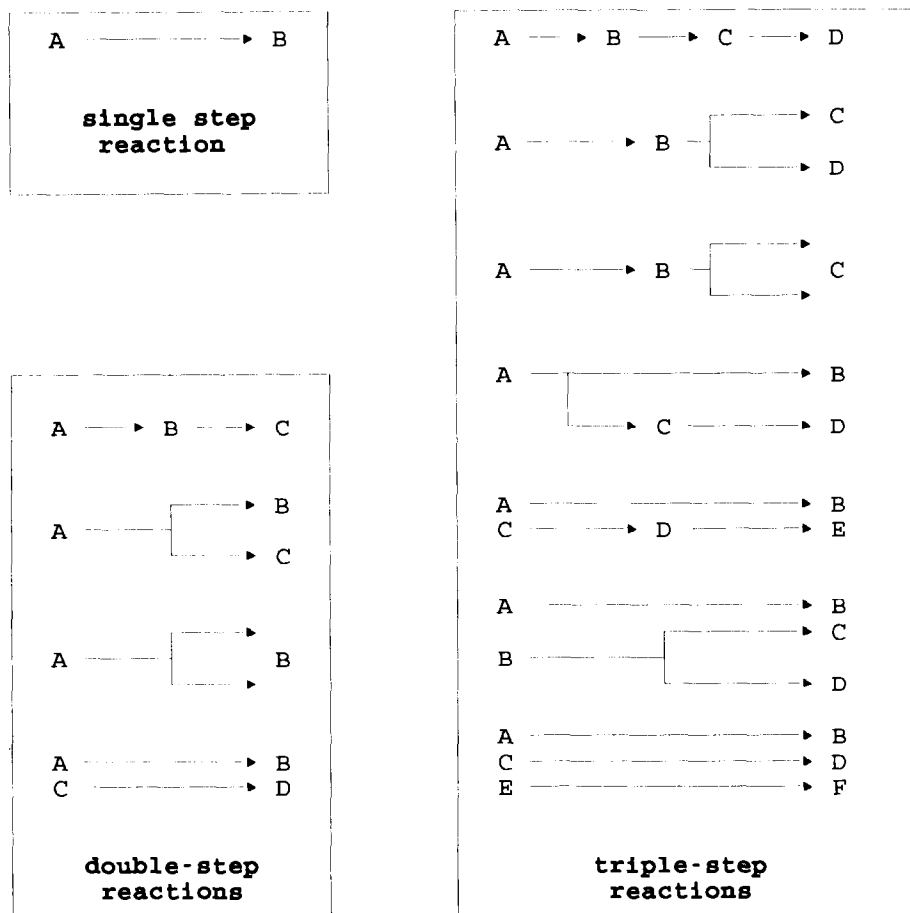


Fig. 1. Set of one to three-step reactions as offered by the programme NETZSCH Thermal Safety Simulations.

3. Basic data for simulation

The simulations are based on data which: (a) contain properties of a substance such as density, heat capacity, thermal conductivity, reaction heat; (b) characterize the reactor by form (sphere, infinite cylinder or infinite plate), radius or thickness; (c) characterize the boundary or start conditions by start temperature, surrounding temperature, heat transmission from the surface; (d) characterize the reaction kinetics of decomposition by the model of the decomposition process, the kinetic parameters. Finally the simulation time range must be fixed.

The following parameters were determined for Zoalen and formed the basis of the simulation:

$\rho = 0.34 \text{ g cm}^{-3}$. It was assumed that the density is equal to that of a poured material, because this best reproduced the pre-melt conditions.

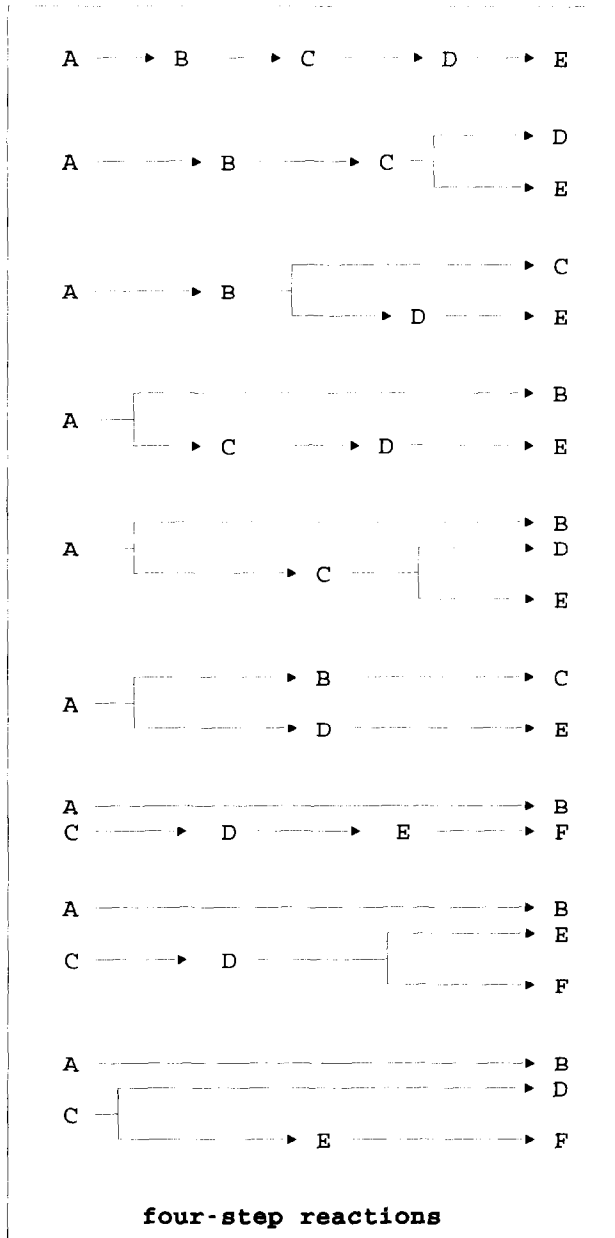


Fig. 2. Set of four-step reactions as offered by the programme NETZSCH Thermal Safety Simulations.

Table 1

Types of reaction and their equations (α = degree of conversion)

Code	$f(\alpha)$	Type of reaction
F1	$(1 - \alpha)$	1st order reaction
F n	$(1 - \alpha)^n$	n th order reaction
D1	$0.5 \cdot \alpha^{-1}$	One-dimensional diffusion
D2	$(-\ln(1 - \alpha))^{-1}$	Two-dimensional diffusion
D3	$1.5 \cdot (1 - \alpha)^{1/3} / [(1 - \alpha)^{-1/3} - 1]$	Three-dimensional diffusion Jander's type
D4	$1.5 \cdot [(1 - \alpha)^{-1/3} - 1]^{-1}$	Three-dimensional diffusion Ginstling-Brounshtein type
R2	$2 \cdot (1 - \alpha)^{1/2}$	Two-dimensional phase boundary reaction
R3	$3 \cdot (1 - \alpha)^{2/3}$	Three-dimensional phase boundary reaction
B1	$\alpha \cdot (1 - \alpha)$	Autocatalysis, Prout-Tompkins
C1	$(1 - \alpha) \cdot (1 + k\text{-cat} \cdot \alpha)$	1st order reaction with auto-catalysis
A2	$2 \cdot (1 - \alpha) \cdot [-\ln(1 - \alpha)]^{1/2}$	Two-dimensional nucleation
A3	$3 \cdot (1 - \alpha) \cdot [-\ln(1 - \alpha)]^{2/3}$	Three-dimensional nucleation
A n	$n \cdot (1 - \alpha) \cdot [-\ln(1 - \alpha)]^{(n-1)/n}$	n -Dimensional nucleation according to Avrami-Erofeev

λ	$0.001 \text{ W (cm K)}^{-1}$. This is an estimated value for organic materials.
c_p	$= 1.34 \text{ W (g K)}^{-1}$
ΔH	$= 3000 \text{ J g}^{-1}$. This value is determined by DSC measurements in an autoclave crucible at a heating rate of 5 K min^{-1} .
$f(c, T)$	The kinetic model was determined by kinetic analysis from DSC measurements both in dynamic and also in isoperibolic mode.

These measurements show that the decomposition process is superimposed by the melting process.

Both processes should first be regarded as being independent of one another. The fact that the melted material has a changed density and a changed thermal conductivity has not been taken into consideration.

In order to guarantee a high level of confidence in the simulation data, dynamic and isoperibolic measurements were carried out at the same time with heat flux calorimeters (DSC). The following will show that a more complex model became necessary for the description, due to the coupling of these different measuring modes.

3.1. DSC measurements and their kinetic analysis

3.1.1. Assessing the measurement

The DSC measurements on Zoalen (Fig. 3) were carried out with three heating rates: 0.5, 1.0 and 2.0 K min^{-1} . They show that, after the melting point at approx. 165°C , the decomposition process is characterized by a peak which has at least two steps. As expected, the maxima of the single peaks shift to higher temperatures when exposed to an increasing heating rate.

3.1.2. Deconvolution of the DSC measurement: transfer correction

Zoalen has such a high vapour pressure in the chosen temperature range that the DSC

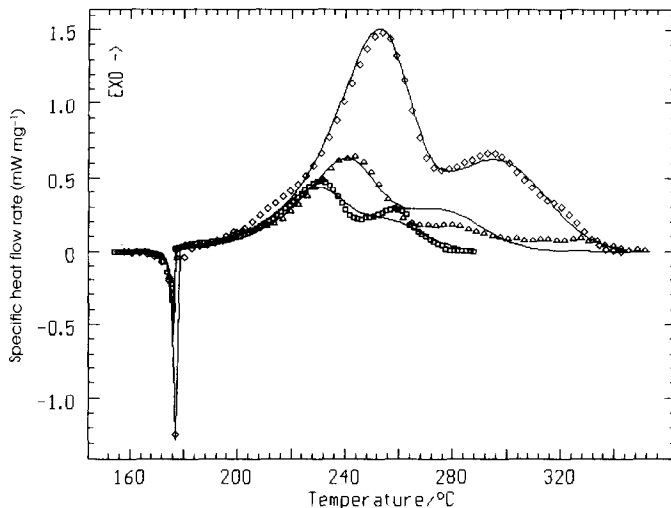


Fig. 3. DSC measurements of Zoalen in an autoclave crucible with results of the fitting by the kinetic model 1. \square , 0.5 K min^{-1} ; \triangle , 1.0 K min^{-1} ; \diamond , 2.0 K min^{-1} .

measurements must be carried out in an autoclave crucible. The DSC signal is greatly deformed (“smeared”) due to the high heat capacity of autoclave crucibles. A correction, the so-called “desmearing” (deconvolution) of the DSC signal (Fig. 4), must therefore be carried out before beginning the kinetic analysis, because kinetic analysis is shown as a peak-form analysis.

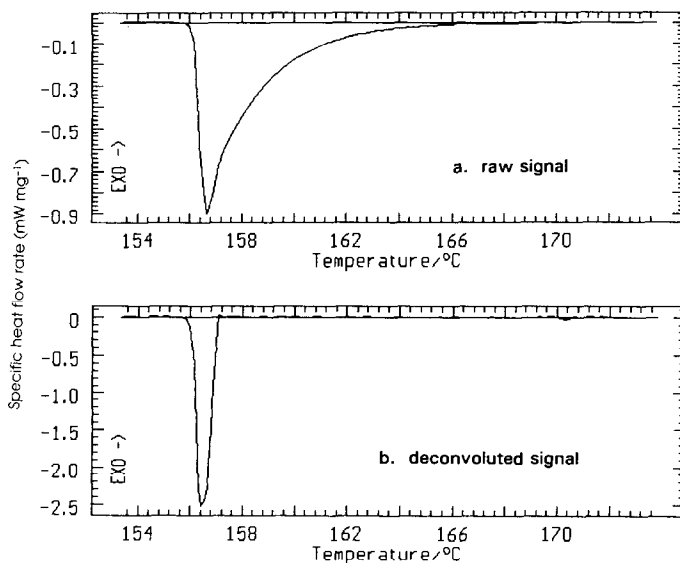


Fig. 4. DSC melting peaks of indium in an autoclave crucible.

The instrument used (a Netzsch-Gerätebau DSC 200) provided the melting peak for indium, using an autoclave crucible as shown in Fig. 4(a). The shape of this signal is typical for autoclave crucibles. It decreases fast after the peak maximum and then returns slowly to the baseline as the time constant increases. The transfer function of the measuring system (cell + autoclave crucible) was determined on the assumption that the deconvoluted DSC signal, after reaching its maximum, returns to the baseline as fast as possible and without overshooting. Fig. 4(b) shows that this was achieved by the selected approximation to a very great extent. Kinetic analysis can only provide relevant parameters once the above has been ensured.

ACTIVATION ENERGIES

Alpha	E kJ/mol		lg A*s
0.98	19.19 +-	44.15	-0.87
0.95	2.24 +-	56.48	-2.65
0.90	-1.87 +-	83.61	-3.17
0.80	51.65 +-	54.32	1.78
0.70	65.43 +-	2.04	3.08
0.60	73.27 +-	13.82	4.07
0.50	91.38 +-	2.07	6.01
0.40	102.33 +-	3.69	7.15
0.30	111.11 +-	0.81	8.04
0.20	117.43 +-	0.28	8.67
0.10	121.54 +-	1.91	9.07
0.05	131.89 +-	5.00	10.19
0.02	141.87 +-	13.20	11.32

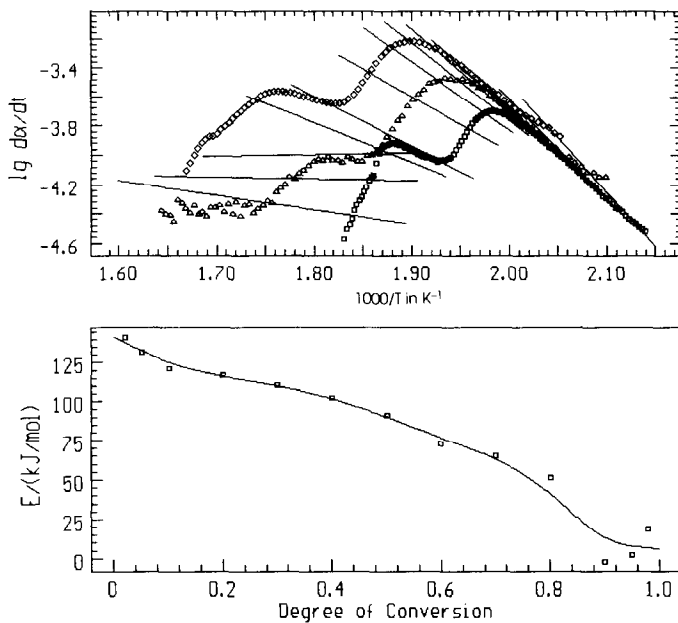


Fig. 5. Friedman analysis of DSC measurements of the thermal decomposition of Zoalen.

3.1.3. Model-free approximation of the activation energy according to both Friedman and Ozawa-Flynn-Wall (OFW)

The DSC measurements in the model-free approximation procedures of the activation energy according to Friedman [12] or Ozawa-Flynn-Wall [13–15] are transformed to the degree of conversion. But, strictly speaking, this conversion is only mathematically correct when used for a one-step reaction process. Therefore this would lead to clearly recognizable errors when used for complex reaction processes. This applies especially to branched reaction models. In spite of this fact, this analysis is carried out because, firstly, one can easily conclude a one-step process from the constancy of the activation energy (a one-tipped peak is no guarantee of a one-step reaction) and secondly because it provides

ACTIVATION ENERGIES				
Alpha	E kJ/mol		lg A*s	
0.98	38.26	+- 28.38	0.48	
0.95	43.30	+- 29.02	0.93	
0.90	59.46	+- 25.98	2.53	
0.80	80.45	+- 9.43	4.67	
0.70	90.47	+- 6.52	5.77	
0.60	105.15	+- 1.53	7.35	
0.50	112.72	+- 0.44	8.15	
0.40	117.44	+- 1.27	8.63	
0.30	121.14	+- 2.02	8.99	
0.20	124.48	+- 2.79	9.32	
0.10	129.11	+- 5.95	9.75	
0.05	131.16	+- 11.05	9.88	
0.02	128.22	+- 13.45	9.33	

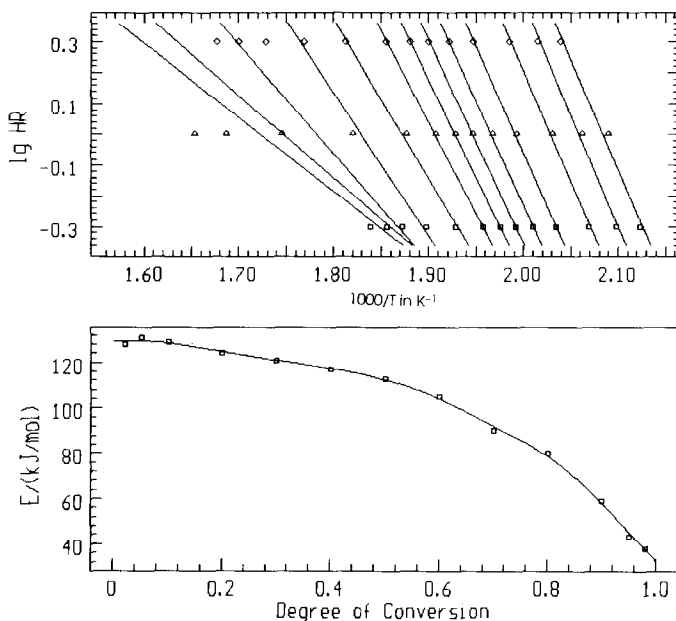


Fig. 6. Ozawa-Flynn-Wall analysis of DSC measurements of the thermal decomposition of Zoalen.

useful assistance in determining the assessed values for the parameters of MULTIVAR-NLR.

One can see from Figs. 5 and 6 that the activation energy does not remain constant within both decomposition peaks. The influence of the previous melting process is still noticeable for small degrees of conversion ($\alpha < 0.1$), whereas large degrees of conversion shift the weighting between the reaction steps according to the heating rate. For this reason one can only carry out a rough estimate: for a degree of conversion up to 0.6, an activation energy of ca. 110 kJ mol^{-1} ; and for over 0.6 an activation energy of ca. 65 kJ mol^{-1} .

3.1.4. Kinetic analysis by means of multivariate non-linear regression (MULTIVAR-NLR)

It is a general statistical principle that a prediction gains in its degree of confidence if the initial data record includes not only the local information but also that from further afield (Fig. 7). If the kinetic analysis is made on the basis of only one dynamic measurement then, to a great extent, this is a case of locally acquired information. However if, in comparison, multiple dynamic measurements are simultaneously analyzed at different heating rates, a larger “global” area of the reaction fields can be acquired by this multivariate data record. Should the adaptation of this data record succeed sufficiently well, then the kinetic parameters which have been determined will allow a high degree of confidence concerning the course of the decomposition reaction, even in a larger range of temperature and time. At the same time, the degree of confidence in predictions concern-

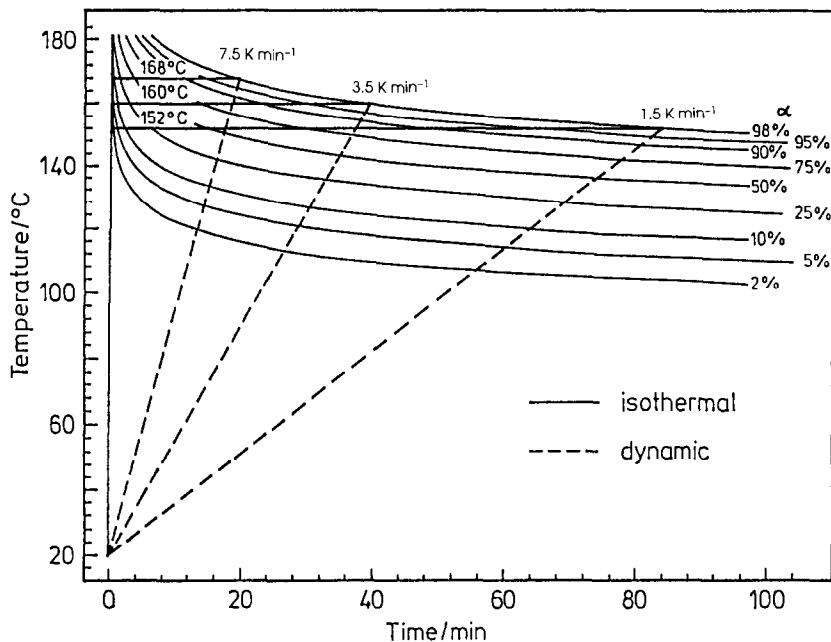


Fig. 7. Presentation of the information of the reaction field with isothermal and dynamic temperature control.

ing areas outside the measuring range will also be clearly diminished as is often the case with simulations of the temporal behaviour of explosive materials. The consequent application of these considerations concerning the kinetic analysis of dynamic DSC measurements is realized by the programme “Netzsch Thermokinetic Analysis, MultipleScan” [9,10]. In this programme, a given kinetic model can be adapted simultaneously to up to six measurements with different heating rates. It is also possible to combine dynamic and isothermal measurements. At the same time, the total course of reaction can consist of up to four reaction steps, whereby the individual reaction steps can have a combined action as independent, competitive or following reactions and each reaction step is characterized by one of the reaction types listed in Table 1.

However, the fitting can only be carried out via non-linear regression (NLR), whereby the relevant differential equations are numerically solved and the parameters of the differential equations are iteratively optimized. Rough starting values for the kinetic parameters, which are necessary for the NLR, can be obtained with all the above-mentioned limitations via the model-free approximation of the activation energy. Because a good starting position is often the deciding factor in the success of a fitting, the optimization by hand proves itself to be extraordinarily useful. By using manual optimization, all parameters can be changed by visual control of the curve fitting. The parameter record is filtered at the same time by the smallest sum of the least squares. The given initial values for the kinetic parameters were usually determined in this way in the following analyses.

The melting process is itself a process of equilibrium. Nevertheless, in order to include this process into the fitting, one would formally describe it as a reaction of broken (small) order with high activation energy (model 1). The melting enthalpy comprises -0.044 of the total peak area.



Within a row of other models, the following types of reaction have proved to be optimum for model 1 (Table 2): *t*: *n*th order; *f*: 1st order with autocat. by C; *f*: 1st order with autocat. by D.

In fact, model 1a provides: *t*: *n*th order; *f*: *n*th order; *f*: *n*th order. This is a slightly, but statistically not significantly better quality of fitting (see Table 3). However, in model 1a the broken reaction orders are not understandable in this model for the following reactions with values around 0.7. Therefore the parameters contained in model 1b will be used later in the simulation.

3.2. Measurements with microcalorimeters in isoperibolic measuring mode

Micro calorimeters that are preferably intended for isoperibolic use, generally have the advantage of a higher absolute sensitivity compared to the heat flux calorimeters used in dynamic measuring mode. This is achieved because the measurement is carried out with an essentially larger sample mass because the temperature measuring system is often develop-

Table 2

Results of the kinetic analysis using MULTIVAR-NLR, model 1b parameters and their standard deviations

No.	Parameter	Optimum value	Standard deviation
0	$\lg_{10}(A1/s^{-1})$	150.0000	Const
1	$E1 \text{ kJ mol}^{-1}$	310.0000	Const
2	React.ord. 1	0.0015	Const
3	$\lg_{10}(A2/s^{-1})$	8.7791	0.5935
4	$E2 \text{ kJ mol}^{-1}$	117.4197	5.1160
5	$\lg_{10} \text{ k-cat } 2$	0.2007	0.1909
6	$\lg_{10}(A3/s^{-1})$	2.7556	0.6703
7	$E3 \text{ kJ mol}^{-1}$	64.9356	5.9182
8	$\lg_{10} \text{ k-cat } 3$	0.3737	0.2774
9	FollReact. 1	-0.0440	Const
10	FollReact. 2	0.6060	0.0235
11	Area 1/(J g^{-1})	2330.7536	91.6526
12	Area 2/(J g^{-1})	1830.2907	69.8636
13	Area 3/(J g^{-1})	2415.1729	40.9149

ed as a multi-thermocouple system. This higher sensitivity has to be paid for by the disadvantage of a slightly lower time resolution so that often no exact statement can be made concerning the kinetics. Because of the above, only a reaction of first order is accepted for the decomposition process. As still no information is known about the current degree of conversion, an evaluation can only be carried out on the assumption of a reaction of zero order.

Fig. 8 shows the results of these measurements with the Thermal Activity Monitor/ThermoMetric, Sweden and with Setaram BT 2.15D/France and their kinetic evaluation. Main results are as follows. One can already observe decomposition far below the melting process. The lower detection limit is, at 45°C, only a little above room temperature. An altered decomposition kinetic begins at the melt (Table 4). If one extrapolates the heat generation both from below as well as from above the melt to the same temperature (180°C), a rapid increase occurs at factor 80.

Table 3

Test to distinguish the fitting quality of models 1a and 1b

Model	f_1	f_{\min}	F_{exp}	$F_{\text{crit}}(0.95)$
1a t : n th order f : n th order f : n th order	407	407	1.00	1.18
1b t : n th order f : 1st order with autocat. by C f : 1st order with autocat. by D	407	407	1.04	1.18

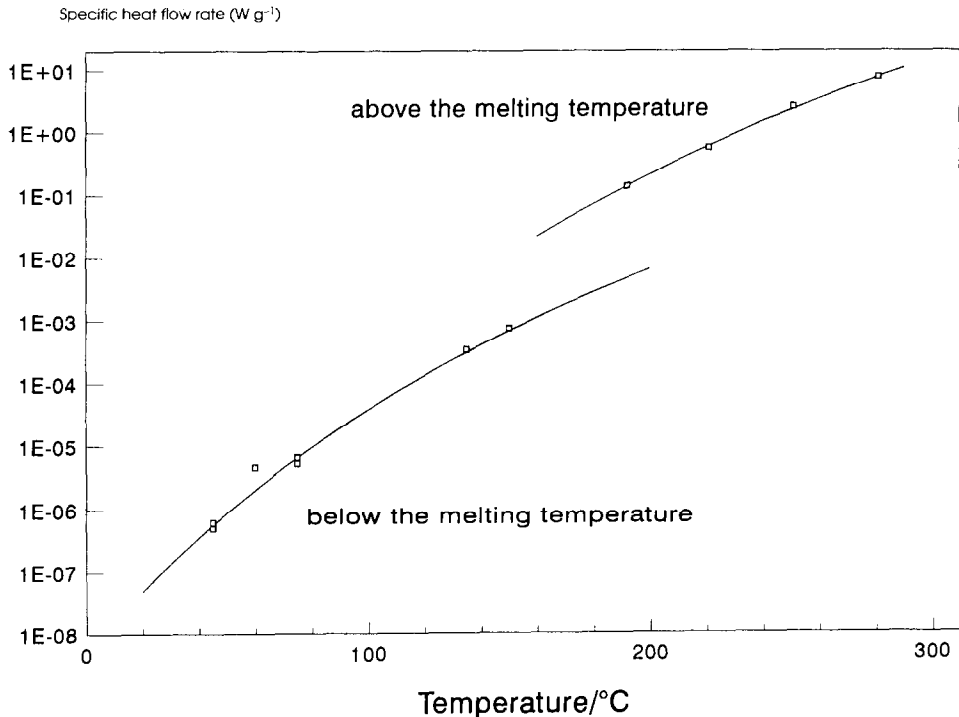


Fig. 8. Measurement of the rate of heat generation in isoperibolic measuring mode below and above the melting temperature of Zoalen.

3.3. Conclusion drawn from the results of DSC measurements in dynamic and isoperibolic measuring mode

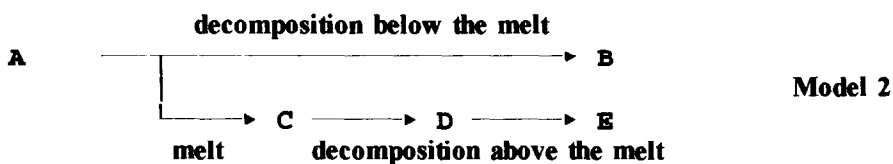
If the decomposition processes that are being carried out at storage temperatures cannot be recorded with the measuring methods used, than this can result in serious misinterpretations. As the example with Zoalen shows, measurements with micro calorimeters in isoperibolic mode are very important, because only they show that decomposition already starts at room temperature. Heat-flux calorimeters in dynamic mode have, it is true, less sensitivity, but they can differentiate fast processes better. For this reason one can characterize the temperature range above the melting temperature better with them.

Table 4

Kinetic data, taken from measurements in isoperibolic measuring mode

Parameter	Below the melting temperature	Above the melting temperature
$\lg(A/s^{-1})$	2.646	6.586
$E/(kJ\ mol^{-1})$	75.313	96.700

Altogether this shows that the results of the simulation achieve a high degree of reliability when one takes advantage of as many sources of information as possible. If one transfers these requirements to the simulation of the decomposition of Zoalen, the following four-step model 2 results from the combination of both measuring methods for the decomposition process:



4. Simulations

First, certain questions are answered by simulations with special conditions. At the same time, the specific behaviour of Zoalen demonstrates a practical example.

4.1. Simulation of the adiabatic case

The adiabatic case is typical in that no conductive heat exchange occurs between the reactor and the surrounding area. The parameter *TransferCoeff.* which determines the conductive heat exchange was therefore set at the very low value of $1.0 \times 10^{-12} \text{ W (cm}^2 \text{ K)}^{-1}$, which is virtually zero.

The result of the simulation is shown by Fig. 9, which entirely lives up to expectations: after a slow, but progressively increasing temperature rise, the entire energy released by the

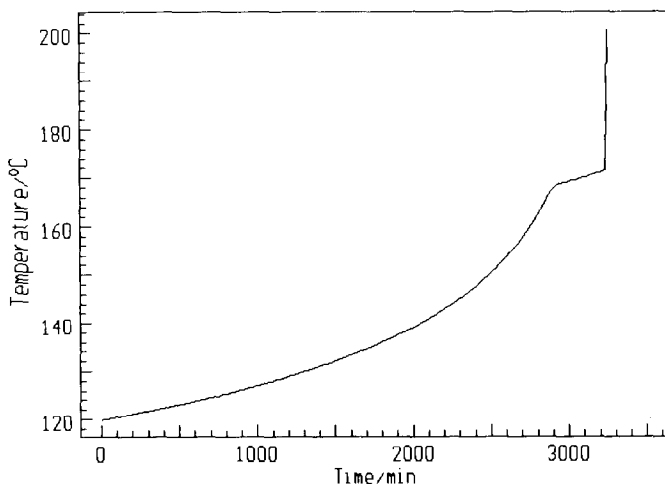


Fig. 9. Simulation of the thermal behaviour of Zoalen in an adiabatic reactor. Model 2; starting temperature 120°C.

decomposition process at the start of the melting process is absorbed by the melting process, so that the temperature remains constant. After the melting process is finished, the decomposition continues explosively. The time which results from the simulation up to the explosion amounts to 3252 min for a starting temperature of 120°C.

4.2. Reactor with heat abstraction via the surface

The reactor with heat abstraction via the surface provides a practical example. By varying the external conditions and by extrapolation, one can determine the boundary conditions in which the potentially explosive material can be stored in a stable state or in which it can be processed. These limiting conditions cannot be calculated analytically from the kinetic parameters of the decomposition kinetics and the external conditions by taking a more complex decomposition process as a basis, in contrast to the simpler models which are based on the theories of Semenov, Frank-Kamenetskii or Thomas. Simulation is the only remaining solution.

Figs. 10–12 show the development of temperature in the reactor for a transfer coefficient of $2 \times 10^{-4} \text{ W (cm}^2 \text{ K)}^{-1}$. It was assumed that, at the beginning, the inner and outer temperatures were exactly the same and amounted to 120°C. One can gather from these figures that up to the time of thermal explosion (a) the temperature on the surface of the reactor hardly exceeded 128°C, and (b) the inner part of the reactor could not be cooled due to the lack of thermal conductivity. Therefore for $r = 0$, i.e. for the centre of the reactor, the same time of initiation was calculated as for the adiabatic case.

In order to determine the boundary conditions valid for Zoalen so that stable storage is provided during cooling (transfer coefficient $\lambda = 0.0002 \text{ W (cm}^2 \text{ K)}^{-1}$), the internal starting temperature and ambient temperature were varied. These conditions are in accordance with

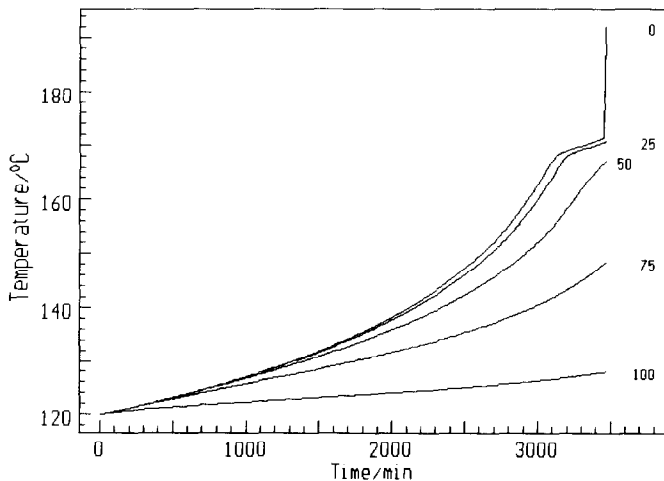


Fig. 10. Simulation of the temperature development of Zoalen in a cylindrical reactor with heat transport over the surface. Model 2; transfer coefficient $0.0002 \text{ W (cm}^2 \text{ K)}^{-1}$; starting temperature 120°C; parameter, relative radial distance in %.

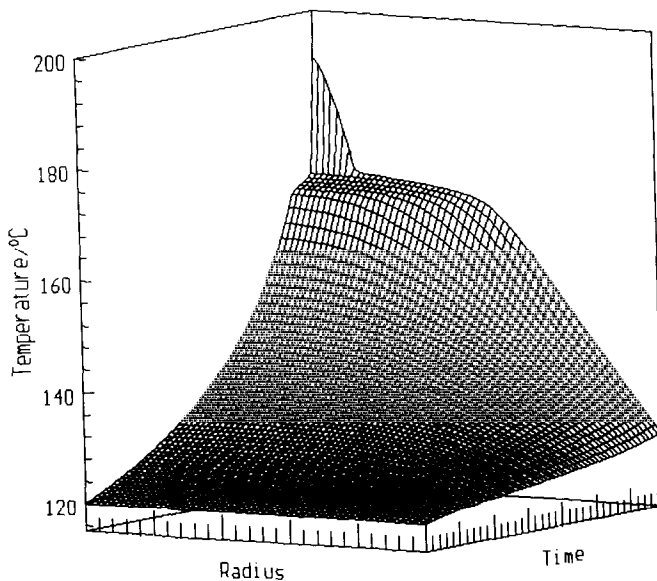


Fig. 11. 3D diagram of the temperature development of Zoalen in a cylindrical reactor with heat transport over the surface. Model 2; transfer coefficient $0.0002 \text{ W (cm}^2 \text{ K)}^{-1}$; starting temperature 120°C .

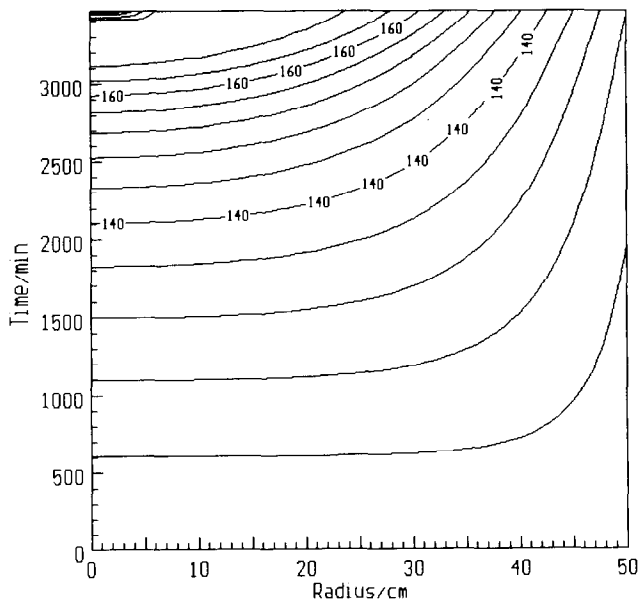


Fig. 12. Isolines of the temperature development of Zoalen in a cylindrical reactor with heat transport over the surface. Model 2; transfer coefficient $0.0002 \text{ W (cm}^2 \text{ K)}^{-1}$; starting temperature 120°C .

Table 5

Data for the determination of the critical storage temperature, which were determined by simulation with model 2

Temperature/°C	Time _{init} /min	10 000 × min/Time _{init}
135	1527	6.549
120	3469	2.883
110	7244	1.380
105	12104	0.826
102	18555	0.539

a reactor, the contents of which are not mixed and the heat of which is only dissipated from the inside by thermal conduction. As one can see from the simulation (Figs. 10–12), the difference between the surface temperature of the reactor and the ambient temperature (below the explosion) is never bigger than 8°C.

The boundary temperature $Temp_{crit}$ for a stable storage is that temperature at which the initiation time tends towards infinity. Instead of determining $Temp_{crit}$ by a time-consuming trial and error procedure, the extrapolation of the inverse initiation time towards zero (Eq. 4) provides the obvious solution:

$$Temp_{crit} = \lim_{1/Time_{init} \rightarrow 0} Temp_{init} \quad (5)$$

Table 5 lists the initiation times which belong to a given starting temperature as well as their reciprocal values. The spline approximation for $1/time_{init} \rightarrow 0$ (Fig. 13) shows a temperature of 96.9°C as the upper boundary value for stable storage.

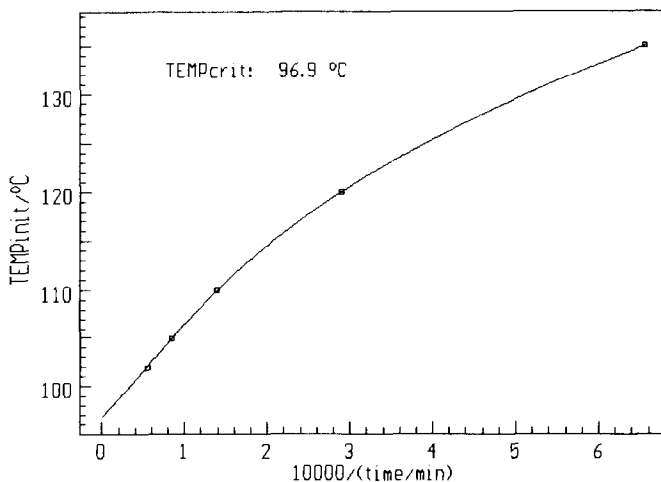


Fig. 13. Extrapolation of the initiation temperature on an inverse initiation time; $10\,000/time_{init} \rightarrow 0$ for model 2.

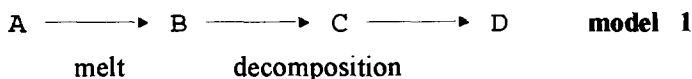
Zoalen provides the rare circumstance in that the results of the simulation have actually been tested by an example from real life. A severe explosion occurred at King's Lynn, UK, in 1976 when using this material. A batch of 1.3 tons blew up by itself 27 h after the end of a drying process. When reconstructing the details of this accident, the assumption was made that the starting temperature had been between 120°C and 135°C. The simulation calculations resulting in Fig. 13 prove this assumption.

4.3. The consequence of insufficient basic data

The following examples show how information can be affected when insufficient or inaccurate basic data are used. While referring to Section 3, models are taken which can ignore certain parts of model 2.

4.3.1. Model without decomposition which starts below the melt

If only basic data of DSC measurements were available, one would have no knowledge of the decomposition which already starts below the melt. The first step of model 1 which was developed by these data is the melting, followed by the decomposition as a two-step reaction.



If one extrapolates for this model the inverse initiation time as a function of the start temperature towards zero, according to Eq. (4), then, as shown in Fig. 14, the thermal runaway only occurs above 156.6°C. This would be an entirely false result and the seeds of the next catastrophe would have been sown.

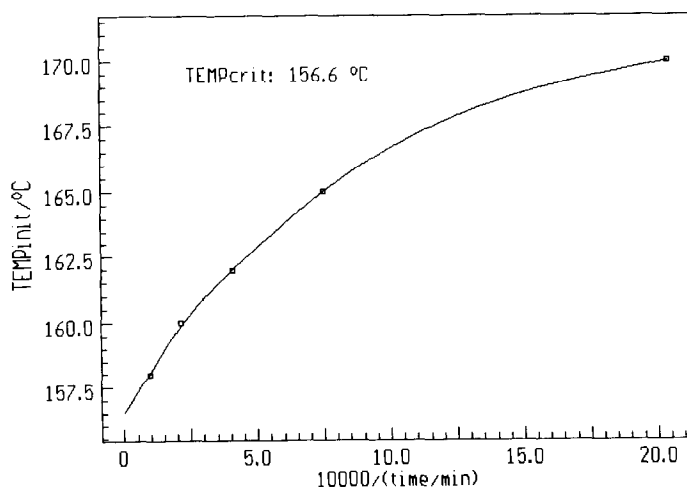


Fig. 14. Extrapolation of the initiation temperature on an inverse initiation time; $10\,000/\text{time}_{\text{init}} \rightarrow 0$ for model 1.

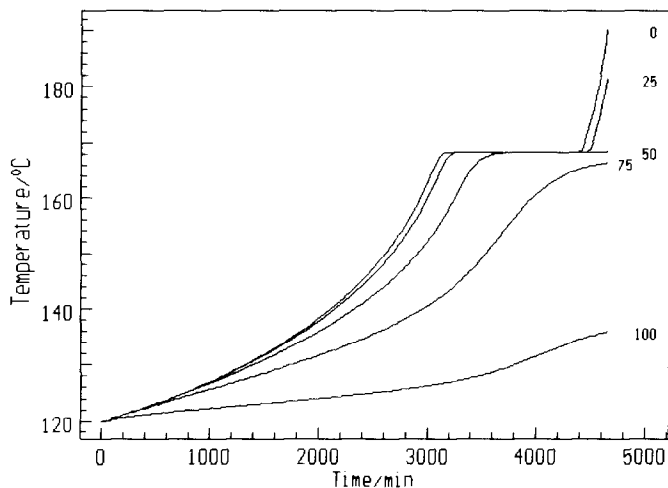
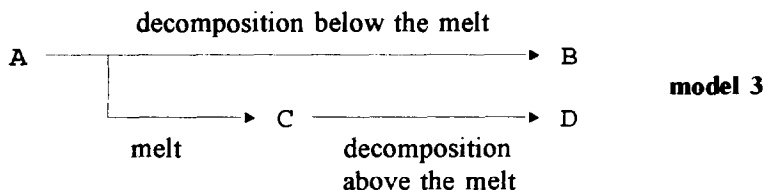


Fig. 15. Simulation of the temperature development of Zoalen in a cylindrical reactor with heat transport over via the surface. Model 3; transfer coefficient $0.0002 \text{ W (cm}^2 \text{ K)}^{-1}$; starting temperature 120°C .

4.3.2. Model without acceleration of the decomposition reaction above the melt

If only the measurements with the isoperibolic calorimeters below the melt were known, then the relevant model 3 would be as follows and the kinetic parameters for reaction $A \rightarrow B$ would be equal to those of the reaction $C \rightarrow D$:



The result of a simulation calculation for the start temperature of 120°C when using model 3, is shown in Fig. 15. Further simulations at different temperatures provided the basic data for Fig. 16. If one compares Fig. 13 with Fig. 16, one sees that the time until the reactor's runaway is prolonged by more than 1000 min, irrespective of the start temperature. The temperature limit for stable storage is, as expected, the same as that for model 2 ($\text{Temp}_{\text{crit}} = 97.0^\circ\text{C}$).

5. Summary

The determination of the critical temperature is an equally important parameter both for the production as well as for the storage of potentially explosive materials. With the help of the extended Thomas theory, realized in the Netzsch-Gerätebau programme, "Thermal Safety Simulations", it is now also possible to determine these parameters for

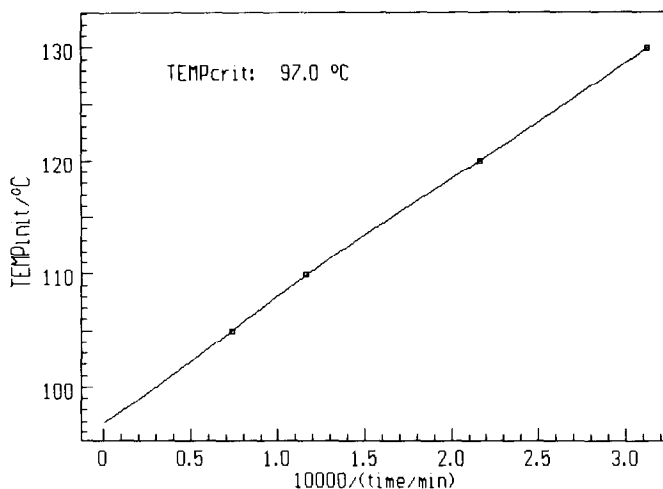


Fig. 16. Extrapolation of the initiation temperature on an inverse initiation time; $10\,000/\text{time}_{\text{init}} \rightarrow 0$ for model 3.

complex decomposition processes. Not only can the decomposition reaction be described by an up to four-step process, which includes follow up, competition and parallel reactions, but the heat conduction equation for the reactor types, infinite plate, infinite cylinder and ball, can be solved at the same time.

The example of Zoalen (3,5-dinitro-*o*-toluamide) shows that by using different measuring methods (dynamic and isoperibolic heat flux calorimetry) the entire complexity of the decomposition is recognizable, and that only by summarizing all this information in a kinetic model can predictions achieve the necessary reliability.

Acknowledgements

We would like to thank Dr. Suter, Sandoz Technologie AG, for checking through this manuscript. His suggestions resulted in a more precise presentation of the entire problem. We would also thank Dr. G. Hentze, formerly Bayer AG, Leverkusen, for his helpful discussions.

References

- [1] H.D. Ferguson, D.I. Townsend, T.C. Hofelich and P.M. Russel, *J. Hazardous Mater.*, 37 (1994) 285–302.
- [2] A.A. Kossov, A.I. Benin, P.Yu. Smykalov and A.N. Kasakov, *Thermochem. Acta*, 203 (1992) 77–92.
- [3] H. Schuler, *Chem.-Ing.-Techn.*, 64 (1992) 975–985.
- [4] J. Verhoeff, *Experimental Study of the Thermal Explosion of Liquids*, Dissert. Techn. Highschool Delft/Netherlands, 1983.
- [5] N. Semenov, *Z. Phys.*, 48 (1928) 571–582.

- [6] N. Semenov, *Einige Probleme der chemischen Kinetik und Reaktionsfähigkeit*, Akademie-Verlag, Berlin, 1961.
- [7] D.A. Frank-Kamenetskii, *Acta Physicochim. URSS*, 10 (1942) No. 3, 365–370.
- [8] P.H. Thomas, *Trans. Faraday Soc.*, 54 (1942) 60–65.
- [9] J. Opfermann, *Manual of the programme "Netzsch Thermokinetic Analysis, MultipleScan"*, Version 6.65, Edition 1994.
- [10] E. Kaisersberger and J. Opfermann, *Laborpraxis*, 4 (1992) 360–364.
- [11] D. Dollimore, *Thermochem. Acta*, 203 (1992) 2–23.
- [12] H.L. Friedman, *J. Polym. Sci.*, C6 (1965) 175.
- [13] T. Ozawa, *Bull. Chem. Soc. Jpn.*, 38 (1965) 1881.
- [14] J.H. Flynn and L.A. Wall, *Polym. Lett.*, 4 (1966) 232.
- [15] J. Opfermann and E. Kaisersberger, *Thermochem. Acta*, 11 (1992) 167.